IL NUOVO CIMENTO **44 C** (2021) 92
DOI 10.1393/ncc/i2021-21092-7

COMMUNICATIONS: SIF Congress 2020

Study of a coronal mass ejection-driven shock in the low solar corona

F. FRASSATI([1]), S. MANCUSO([1]), A. BEMPORAD([1]) and D. BARGHINI([1])([2])

([1]) *INAF, Osservatorio Astrofisico di Torino - via Osservatorio 20, Pino Torinese, Italy*
([2]) *Università degli Studi di Torino, Dipartimento di Fisica - via P. Giuria 1, Torino, Italy*

received 15 January 2021

Summary. — The characterization of coronal shock waves driven by energetic coronal mass ejections (CMEs) is an important topic in solar physics. In this work, we explore how the analysis of simultaneous data obtained from both extreme ultraviolet (EUV) and radio observations can be successfully used to investigate the physics of CME-driven shocks in the low solar corona. In particular, we analyzed EUV and radio observations of an eruption that propagated above the solar limb on 2014 October 30 and was accompanied by a type-II radio burst, which represents the signature of a coronal shock wave. The analysis of the combined EUV and radio data allowed us to unravel the controversial origin of band-splitting in type-II radio bursts. Moreover, we obtained estimates of important plasma parameters, such as the density compression ratio and the plasma temperature. Finally, the geometry of the CME/shock event was recovered through data-driven 3D modelling.

1. – Introduction

The Sun exhibits a strong dynamic behaviour at all spatial and temporal scales and its surface and atmosphere are subject to continuous changes. The most violent and spectacular phenomena can be categorized as follows:

- *prominences*: quiescent or eruptive bright structures extending up to thousands of km above the solar surface, characterized by high-density and low-temperature chromospheric plasma;
- *solar flares*: sudden increases in brightness observed at all wavelengths (but particularly in the X-ray band);
- *coronal mass ejections (CMEs)*: sudden expulsions of huge amounts of magnetized plasma (up to 10^{16} g) with speeds ranging from about 500 km s^{-1} up to 2500 km s^{-1} and temperatures around 10^6 K;
- *shock waves*: CMEs faster than the local magnetosonic speed can drive magnetohydrodynamics (MHD) shocks that accelerate charged particles to very high energies in the interplanetary space.

- *type-II radio bursts*: energetic electrons accelerated at shock fronts are unstable to Langmuir waves and can get converted into radio emission at the local plasma frequency ($f_{pe} \approx 0.009\sqrt{n_{\rm e}[{\rm cm}^{-3}]}\,{\rm MHz}$) and its harmonic, thus producing characteristic bands of emission in radio dynamic spectra that slowly drift from high to low frequencies;
- *solar energetic particles (SEPs)*: energetic electrons, protons and heavier ions detected in the interplanetary medium with energy ranging from keV to GeV.

In space, shocks are associated with major perturbations that may cause severe geomagnetic storms and SEPs, which in turn can pose significant radiation hazards for astronauts and technological systems orbiting beyond the Earth. The mutual causal relationships between these different phenomena are far from being fully understood. Understanding the dynamics of solar eruptions, the evolution of interplanetary (IP) shocks, and the origin and acceleration mechanism of SEPs is thus of paramount importance in space weather.

2. – A case study

On 2014 October 30, at around 13 UT, an eruption occurred at the eastern limb of the Sun (fig. 1, left panel) in active region NOAA 12201, involving a moderate soft X-ray flare and a CME, which was detected higher up in the corona in white-light (WL) coronagraph images (fig. 1, middle panel). The radio signature of the shock was detected as a type-II radio burst by ground-based radio spectrometers (fig. 1, right panel).

2˙1. *Radio data analysis*. – Type-II radio bursts represent the clearest signatures of shock waves travelling outward in the corona. For this event, two consecutive episodes of band-splitting of the type-II harmonic band were observed. The first one was analyzed by using ground-based radio dynamic spectra combined with multi-wavelength images from the Nançay Radio Heliograph (NRH). A 3D data-driven model was implemented by [1] to ascertain that the band-splitting episode was due to the intersection of the expanding

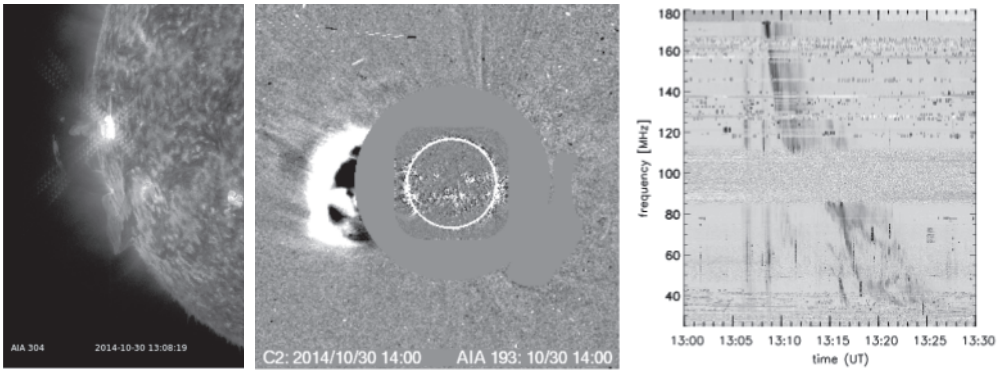

Fig. 1. – Left: solar prominence eruption and flare as seen by SDO/AIA at 304 Å; middle: combined running difference images of the SOHO/LASCO C2 WL coronagraph and SDO/AIA at 193 Å; Right: metric dynamic radio spectrum from the Radio Solar Telescope Network (RSTN) data archive (`https://www.ngdc.noaa.gov/stp/space-weather/solar-data/solar-features/solar-radio/rstn-spectral/`).

shock front with two different adjacent streamers (see [2]). The second episode of band-splitting was instead ascribed to simultaneous emission from pre-shock upstream (U) plasma and compressed downstream (D) plasma (see [3]). This allowed us to obtain the density compression ratio $X_{\rm radio} = \left(\frac{f_{\rm U}}{f_{\rm D}}\right)^2 \approx 1.1$–$1.4$, where f is the observed frequency.

2˙2. *EUV data analysis.* – EUV waves (or EIT waves) are related to the early phases of CMEs. They are also called coronal bright front [4] and recent studies have confirmed that they can be MHD waves or shocks [5,6]. This event shows an EUV expanding front clearly visible in 171 Å, 193 Å, and 211 Å filters, corresponding to coronal temperatures in the range $T \approx 1.6$–4.0 MK. By analyzing the EUV data, we were able to infer the location of the shock sheath, formed behind the shock, thanks to the increase of the EUV intensity above the background signal around the onset of the type-II radio emission (see details in [3]). The EUV intensity measurements were also used to quantify the emission measure $EM(\Delta T)$ (eq. (1a)), representing the total amount of emitting material as a function of the coronal plasma temperature along the line of sight (LOS), and the electron density upstream and downstream of the expanding front (eq. (1b)). This allowed us to estimate the electron density compression ratio $X_{\rm EUV}$ (eq. (1c)) (by adapting the calculation of the compression ratio X made by [7] for WL data to the analysis of EUV observations) at a given plasma temperature range ΔT:

$$EM(\Delta T) = \int_{\Delta T} \frac{{\rm d}EM(T)}{{\rm d}T} {\rm d}T, \tag{1a}$$

$$n_{\rm e} \simeq \sqrt{\frac{EM}{s}}, \quad s \sim \sqrt{H \pi r}, \tag{1b}$$

$$X_{\rm EUV} = \sqrt{\frac{EM_{\rm D} - EM_{\rm U}}{P_{\rm U}} + 1} \approx 1.15\text{–}1.23, \qquad \text{for } T = 2.0\text{–}3.0 \text{ MK}. \tag{1c}$$

In the above equations, $P_{\rm U} = L\langle n^2_{\rm e,U}\rangle_{\rm LOS}$, where L is the extension of the plasma region along the LOS, s is the effective LOS path length, H is the hydrostatic scale height, and r is the heliocentric distance (see details in [8,9]). The compression ratio $X_{\rm EUV}$ was calculated as a function of temperature and time. By comparing $X_{\rm radio}$ and $X_{\rm EUV}$, we found a good agreement in the temperature range $T \approx 2$–3 MK, thus supporting the interpretation that the emitting plasma observed in the EUV images is the same plasma that is responsible for the type-II radio emission. This also suggests that the observed EUV front was a CME-driven shock wave.

2˙3. *3D reconstruction of CME-driven shock-streamer interaction.* – Coronal shocks detected by SDO/AIA generally appear, at least in their initial stage, as projections of bubble-like structures in the plane of the sky. Under the above assumption and by using as constraints both EUV and radio heliograph images, the 3D evolution of the expanding shock front (fig. 2) was modelled with a data-driven approach. This also allowed us to investigate, as already mentioned, the exact physical mechanism responsible for the observed band-splitting of the type-II radio emission (see [1] for a complete discussion).

3. – Conclusions

The origin of band-splitting in type-II radio bursts is still a controversial issue and has been mainly interpreted in the past decades as a) originating from the intersection of

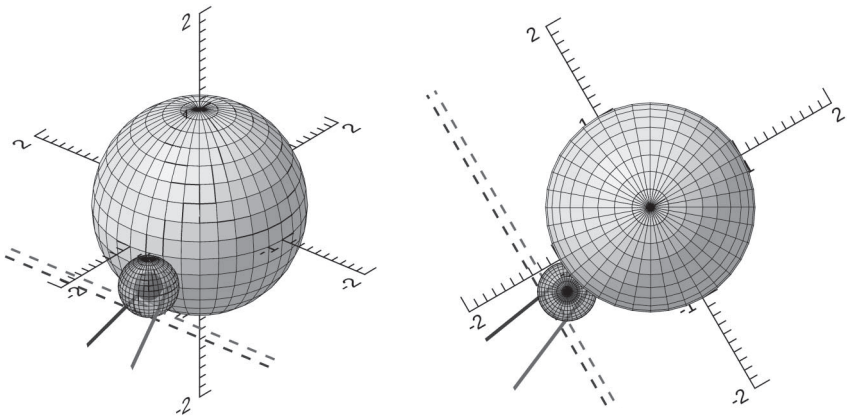

Fig. 2. – 3D model of the CME (inner dark grey sphere)/shock surface (outer lighter grey sphere) interacting with two streamers as seen from two different perspectives. The bigger sphere represents the Sun; the dashed lines denote two LOSs.

the propagating shock with adjacent coronal streamer structures and/or b) as due to the simultaneous emission of radiation from the ambient and compressed plasma upstream and downstream, respectively, of the expanding shock front.

The EUV and radio analysis of the event outlined in this work presented an unprecedented opportunity to confirm that the origin of the observed band-splitting in type-II radio bursts can be actually attributed to both the above cases, depending on the local conditions in the coronal environment. Furthermore, this study allowed us to obtain indirect estimates of both the CME-driven coronal shock spatio-temporal evolution and of important plasma properties, such as the electron density compression ratio and the plasma emitting temperature. The complete analysis of this event, together with a thorough discussion of the results, can be found in [1, 3].

* * *

The authors would like to thank the teams of e-Callisto, NRH, and SDO/AIA for their open-data use policy. FF is supported by the Metis programme funded by the Italian Space Agency (ASI) under the contracts of the co-financing National Institute of Astrophysics (INAF): Accordo ASI-INAF no. 2018-30-HH.0.

REFERENCES

[1] Mancuso S., Frassati F., Bemporad A. and Barghini D., *Astron. Astrophys.*, **624** (2019) L2.
[2] Mancuso S. and Raymond J. C., *Astron. Astrophys.*, **413** (2004) 363.
[3] Frassati F., Mancuso S. and Bemporad A., *Sol. Phys.*, **295** (2020) 124.
[4] Long D. M., DeLuca E. E. and Gallagher P. T., *Astrophys. J.*, **741** (2011) L21.
[5] Patsourakos S. and Vourlidas A., *Sol. Phys.*, **281** (2012) 187.
[6] Long D. M., Bloomfield D. S., Chen P. F., Downs C., Gallagher P. T., Kwon R. Y., Vanninathan K., Veronig A. M., Vourlidas A., Vršnak B., Warmuth A. and Žic T., *Sol. Phys.*, **292** (2017) 7.
[7] Bemporad A. and Mancuso S. *Astrophys. J.*, **720** (2010) 130.
[8] Hannah I. G. and Kontar E. P., *Astron. Astrophys.*, **539** (2012) A146.
[9] Frassati F., Susino R., Mancuso S. and Bemporad A., *Astrophys. J.*, **871** (2019) 212.